Available online at www.sciencedirect.com
ScienceDirect
Advances in Space Research 41 (2008) 1454–1458
ADVANCES IN SPACE RESEARCH
(a COSPAR publication)
www.elsevier.com/locate/asr

Case studies of height structure of TID propagation characteristics using cross-correlation analysis of incoherent scatter radar and DPS-4 ionosonde data

K.G. Ratovsky *, A.V. Medvedev, M.V. Tolstikov, D.S. Kushnarev

Institute of Solar-Terrestrial Physics, P.O. Box 4026, Irkutsk, 33, 664033, Russia

Received 27 October 2006; received in revised form 17 January 2007; accepted 5 March 2007

Abstract

The height structure of TID characteristics is studied on the base of the electron density profiles measured by two beams of the incoherent scatter radar and DPS-4 ionosonde. The height profiles of the TID propagation characteristics are obtained by means of cross-correlation and spectrum analysis of the radar and ionosonde data. The noticeable height variability of the TID parameters is observed. The variability is explained by interference of several TIDs. The obtained TID propagation characteristics are compared with known results of the TID studies.
© 2007 COSPAR. Published by Elsevier Ltd. All rights reserved.

Keywords: Traveling ionospheric disturbances; Incoherent scatter radar; DPS-4 ionosonde; Propagation characteristics; Height variability; Interference

1. Introduction

The phenomenon of atmospheric gravity waves (AGW) and their ionospheric manifestation, travelling ionospheric disturbances (TID), have been studied both experimentally and theoretically since the 1960s. Recent theoretical studies are developed in the directions of numerical simulation of AGW generation and propagation (Ahmadov and Kunitsyn, 2004) and interrelations between AGW and TID characteristics (Kirchengast, 1996). Experimental progress is associated with measurements of most complete set of TID parameters.

For studying the both vertical and horizontal structure of TIDs we have to measure height profiles of ionospheric parameters at horizontally separated points. Such measurements were made using multiple beams of EISCAT (Ma et al., 1998) and MU radar (Oliver et al., 1988). Herewith only Ma et al. (1998) have investigated the complete wave propagation vector of TIDs as function of height. In this paper the case studies of TID propagation characteristics using cross-correlation analysis of the incoherent scatter radar (ISR) (Zherebtsov et al., 2002) and DPS-4 ionosonde (Reinisch et al., 1997) data are presented. The both tools are located near Irkutsk (52.5N, 104.3E, LT = UT + 7). The ISR antenna system allows beam steering in the plane passing through the major axis of the antenna. As a beam lying out of this plane we used the ionosonde measurements. The ISR and DPS-4 positions and the ground projections of two ISR beams are shown in Fig. 1.

The experimental data are the electron density profiles measured by two ISR beams depicted in Fig. 1 and by DPS-4 ionosonde. The distinctive property of the Irkutsk ISR implies that the electron density profile is measured by the Faraday rotation method (Shpynev, 2004) and hence ISR has no need of calibration by ionosonde. All DPS-4 ionograms have been manually scaled with the interactive ionogram scaling technology described by Reinisch et al. (2004). The electron density profiles were constructed from the ionogram traces using the Reinisch and Huang (1983) method with the extrapolation above a peak height (Reinisch and Huang, 2001).

* Corresponding author.
E-mail address: ratovsky@iszf.irk.ru (K.G. Ratovsky).

0273-1177/$34 © 2007 COSPAR. Published by Elsevier Ltd. All rights reserved.
doi:10.1016/j.asr.2007.03.008

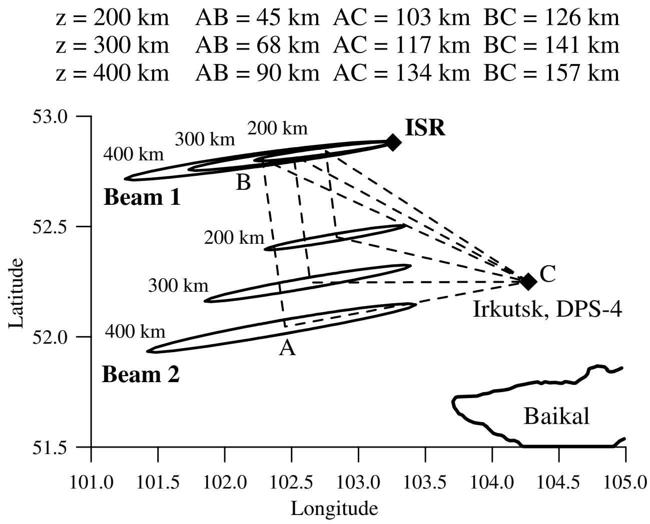

Fig. 1. Positions of ISR and DPS-4. Ground projection of two ISR beams at heights of 200, 300 and 400 km.

For the analysis we selected magnetically disturbed day of September 11, 2005. The $\sum K_p$ was 50^+, K_p index was not less than 6^+ for 0–15 UT interval and reached its peak of 8^- on 6–9 UT interval.

2. Analysis method

As mentioned above, the data are the electron density (Ne) profiles measured by two beams of ISR and by DPS-4 ionosonde. The Ne-TIDs were selected from Ne diurnal variations by band-pass filtering with period band of 1–4 hour. The selected Ne-TIDs are shown in Fig. 2.

We assume that Ne-TIDs have the form of planar wave:

$$\Delta \mathrm{Ne}(\vec{R},t) = \Delta N_0(z) A(t-\tau(\vec{R})), \quad (1)$$

where $\Delta N_0(z)$ is height profile of TID, $A(t)$ is its temporal form,

$$\tau(\vec{R}) = (\vec{e}\cdot\vec{R})/V, \quad (2)$$

$\vec{R} = \{R_x, R_y, R_z\}$ is radius-vector of observation point, $\vec{e} = \{e_x, e_y, e_z\}$ is unit vector specifying the wave propagation direction, V is wave velocity. As a coordinate system we chose Cartesian system with the origin in ISR location, where the z-axis is upward, the x-axis is northward, y-axis is eastward. In this system the $\vec{e}$ vector has the coordinates $\{\cos\theta\cos\psi,\ \cos\theta\sin\psi,\ \sin\theta\}$, where θ is elevation angle over the horizon with upward wave propagation direction as a positive, ψ is azimuth angle with respect to north, taking clockwise as a positive.

The delay (or time difference) between the Ne-TIDs observed at the points with radius-vectors $\vec{R}_1$ and $\vec{R}_2$ is

$$\Delta\tau(\vec{R}_1,\vec{R}_2) = (\vec{q}\cdot(\vec{R}_1-\vec{R}_2)), \qquad \text{where } \vec{q} = \vec{e}/V. \quad (3)$$

Using the mutual delays between the Ne-TIDs observed by two beams of ISR and DPS-4 at the same heights we obtain

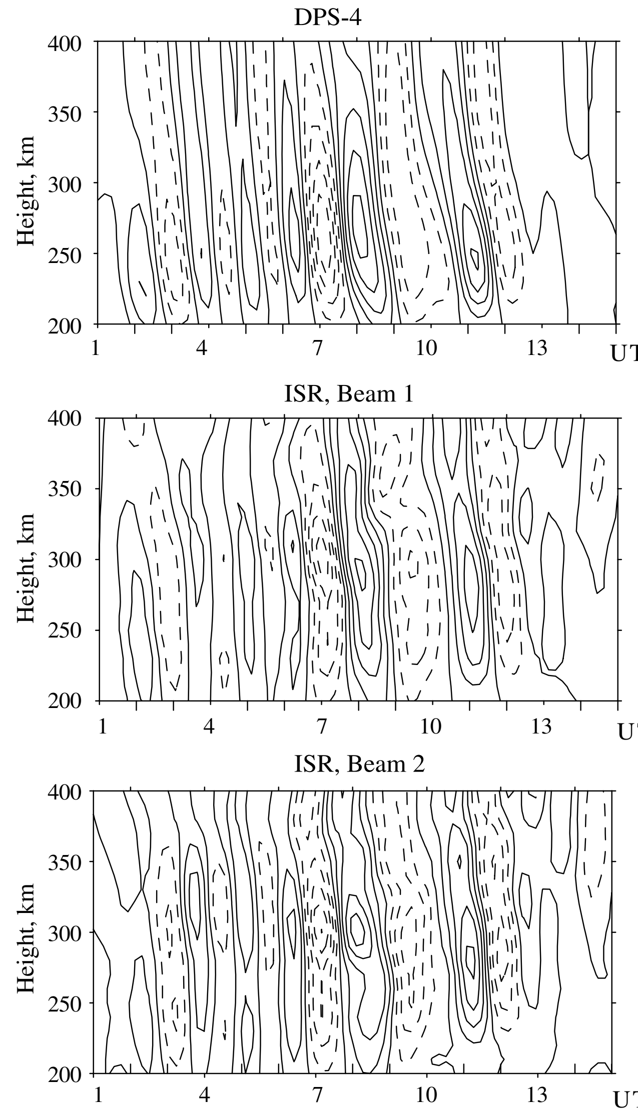

Fig. 2. Ne-TIDs within a period band of 1–4 h. September 11, 2005. LT = UT + 7. Positive contours are solid lines and negative contours are dashed. The contour step is $0.4\times10^{11}\ \mathrm{m}^{-3}$.

the linear system of equations for determination of q_x and q_y:

$$\begin{cases} q_x(x_1-x_2)+q_y(y_1-y_2) = \Delta\tau_{12} \\ q_x(x_2-x_3)+q_y(y_2-y_3) = \Delta\tau_{23} \\ q_x(x_3-x_1)+q_y(y_3-y_1) = \Delta\tau_{31} \end{cases} \quad (4)$$

where (x_1,y_1), $(x_2,\ y_2)$ and (x_3,y_3) are observing points coordinates in xy-plain for two beams of ISR and DPS-4, respectively. By solving this system we obtain the expressions for q_x and q_y

$$\begin{cases} q_x = (\Delta\tau_{12}(\Delta y_{23}-\Delta y_{31})+\Delta\tau_{23}(\Delta y_{31}-\Delta y_{12}) \\ \quad +\Delta\tau_{31}(\Delta y_{12}-\Delta y_{23}))/3S \\ q_y = -(\Delta\tau_{12}(\Delta x_{23}-\Delta x_{31})+\Delta\tau_{23}(\Delta x_{31}-\Delta x_{12}) \\ \quad +\Delta\tau_{31}(\Delta x_{12}-\Delta x_{23}))/3S \end{cases} \quad (5)$$

where $\Delta x_{ij} = x_i - x_j$, $\Delta\ y_{ij} = y_i - y_j$, $S = \Delta x_{12}\Delta y_{23} - \Delta x_{23}\text{-}\Delta y_{12}$ is doubled area of the triangle having apexes (x_1, y_1), (x_2, y_2) and (x_3, y_3). Using the delays $\Delta\tau_z$ between the Ne-TIDs observed by DPS-4 at different heights we can determinate q_z:

$$q_z = \Delta\tau_z/\Delta z. \tag{6}$$

From complete $\vec{q}$ vector one can calculate the TID characteristics V, θ, ψ for different heights.

In particular case when Ne-TID has the form of monochromatic planar wave we can determinate the complete wave vector $\vec{k}\cdot$ and associated characteristics V, θ, ψ using the equations analogous to Eqs. (5) and (6) for phase difference $\Delta\varphi$ between harmonics observed at different points:

$$\begin{cases} k_x = (\Delta\varphi_{12}(\Delta y_{23} - \Delta y_{31}) + \Delta\varphi_{23}(\Delta y_{31} - \Delta y_{12}) \\ \qquad + \Delta\varphi_{31}(\Delta y_{12} - \Delta y_{23}))/3S \\ k_y = -(\Delta\varphi_{12}(\Delta x_{23} - \Delta x_{31}) + \Delta\varphi_{23}(\Delta x_{31} - \Delta x_{12}) \\ \qquad + \Delta\varphi_{31}(\Delta x_{12} - \Delta x_{23}))/3S \\ k_z = \Delta\varphi_z/\Delta z \end{cases} \tag{7}$$

For the determination of the TID propagation characteristics we used two methods. The first one (cross-correlation method) involved the determination of the delays between the TIDs observed at different points by the cross-correlation analysis. Thereafter the TID characteristics were calculated using Eqs. (5) and (6). The second method (phase difference method) involved the TID spectrum analysis on the base of FFT, selection of dominant harmonic and determination of the phase difference between harmonics observed at different points. Thereafter the TID characteristics were calculated using Eq. (7).

3. Results and discussion

Fig. 3 shows the TID propagation azimuth as a function of time and height. The values were calculated by cross-correlation method with 1.5 h length of time series. One can see that the azimuth as a whole varies considerably with height and time. Only for 2–4 UT interval in 230–370 km height range and for 10–12 UT interval in 280–380 km height range the azimuth is approximately constant with height.

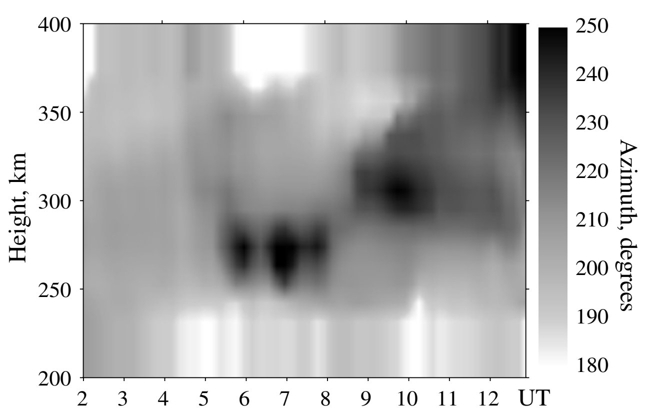

Fig. 3. The results of azimuth calculation by cross-correlation method.

In our opinion the azimuth variability is due to interference of several TIDs. We attempted to separate the TIDs using TID spectrum analysis. The contours of the power spectral density calculated for two intervals are shown in Fig. 4. The analysis exhibited the dominant harmonic with period of 1.5 h for 2:30–5:30 UT interval and the dominant harmonic with period of 2.8 h for 7:00–12:30 UT interval. Using only the dominant harmonics we calculated height profiles of the wave propagation characteristics by phase difference method. These profiles are shown in Fig. 5 together with results obtained by cross-correlation method with time series equal to spectrum analysis intervals.

It can be seen from Fig. 5a that both methods give close results. It implies that the Ne-TID observed from 2:30 to 5:30 UT has a good approximation by one harmonic. It can also be seen from Fig. 5a that the azimuth and velocity magnitude vary slightly with height, whereas the elevation changes strongly. It looks like an interference of two waves with the same azimuths, frequencies and velocities but with different elevations.

Fig. 5b shows that the results obtained by two methods are not in a good agreement for the elevation and velocity magnitude. It can be seen from Fig. 4 that there are two harmonics with periods of 2.8 and 1.5 h in the spectrum for 7:00–12:30 UT interval. The existence of 1.5 h harmonic markedly affects the results of cross-correlation method and appears only slightly in the results of phase difference method because of spectrum separation of harmonics. Nevertheless even for this method the azimuth changes strongly with height, while elevation variability is small enough. Most likely we observe an interference of two waves with the close frequencies and elevations but with different azimuths (e.g. an interference of waves from different sources).

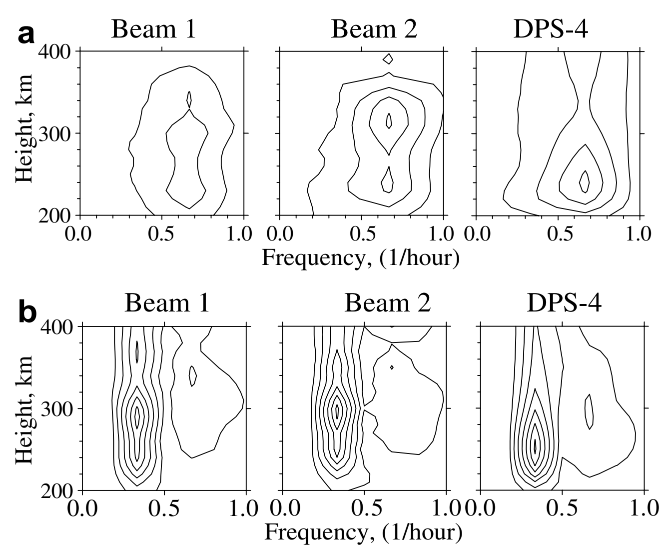

Fig. 4. The contours of the power spectral density. (a) for 2:30–5:30 UT interval, (b) for 7:00–2:30 UT interval.

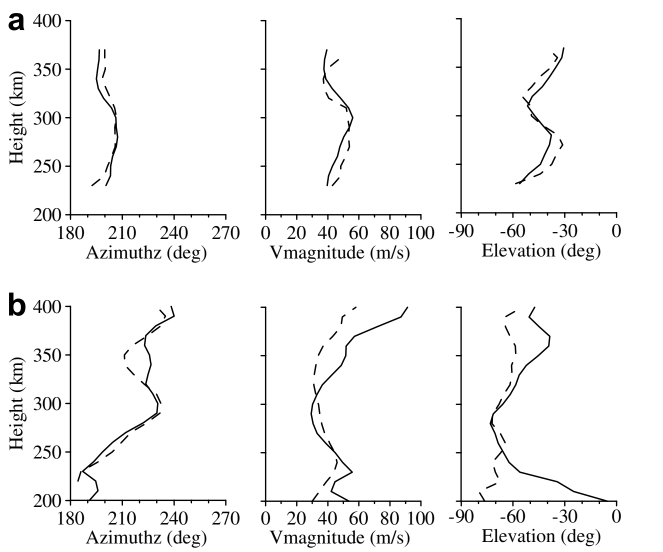

Fig. 5. The height profiles of the TID characteristics calculated by cross-correlation (solid line) and phase difference (dashed) methods. (a) The analysis interval is 2:30–5:30 UT. The dominant harmonic period is 1.5 h (b) The analysis interval is 7:00–12:30 UT. The dominant harmonic period is 2.8 h.

In our opinion the height variability of characteristics is due to interference of several TIDs. Therefore the TID separation methods should be developed. In our studies we used the method of temporal separation (cross-correlation method) and the method of spectral separation the base of FFT (phase difference method). Neither of two methods provides the complete TID separation. Ma et al. (1998) applied the maximum entropy cross-spectral analysis for studying TID propagation characteristics. However, according to their studies, the noticeable height variability of wave vector components was observed, which in our opinion is due to interference of several TIDs.

We compared our measurements with known results of the TID studies (Ma et al., 1998;Oliver et al., 1988; Hocke and Schlegel, 1996; Williams et al., 1982). As estimations of characteristics we took height average values. For the first disturbance observed from 2:30 to 5:30 UT (9:30–12:30 LT) the period T_1 is 1.5 h, the phase velocity magnitude V_1 is 45 ± 8 m/s, the elevation over the horizon θ_1 is $-45° \pm 14°$ and the azimuth ψ_1 is $201° \pm 6°$ ($\pm$ indicates the height variability). For the second disturbance observed from 7:00 to 12:30 UT (14:00–19:30 LT) the estimations are: $T_2 = 2.8$ h, $V_2 = 44 \pm 14$ m/s, $\theta_2 = -70° \pm 10°$, $\psi_2 = 210° \pm 25°$.

The obtained southward and downward propagation of the phase front is the typical large scale TID feature (Hocke and Schlegel, 1996). The phase velocity magnitude values are closer to the results obtained by Ma et al. (1998) ($V = 50$ m/s) and Williams et al. (1982) ($V = 62$ m/s) than to those obtained by Oliver et al. (1988) ($V = 80$ m/s) and reported in the Hocke and Schlegel (1996) review ($V = 96$–113 m/s). Increasing absolute value of elevation angle $|\theta|$ with wave period is in agreement with Hines (1960) dispersion equation for atmospheric gravity waves, whereas the $|\theta|$ values look underestimated compared to those reported in the papers of Ma et al. (1998) ($|\theta| = 74°$), Williams et al. (1982) ($|\theta| = 74°$), Oliver et al. (1988) ($|\theta| = 79°$) and Hocke and Schlegel (1996) ($|\theta| = 72° \div 82°$). One of reasons for underestimating $|\theta|$ can be the impact of TIDs interference upon the obtained results.

4. Conclusion

For the first time the height structure of TID propagation characteristics have been investigated on the base of Ne height profiles measured by ISR and DPS-4 ionosonde using cross-correlation and phase difference methods.

We compared our measurements with known results of the TID studies. The obtained southward and downward propagation of the phase front and increasing absolute value of elevation angle with wave period are in agreement with known TID features, whereas the elevation angle magnitudes look underestimated compared to the results of other researchers. This discrepancy can be caused by the interference of several TIDs.

In our opinion the interference manifest itself in the height variability of TID propagation characteristics. The noticeable height variability of wave parameters was also observed by Ma et al. (1998) and Lanchester et al. (1993). If the interference of several TIDs is a typical phenomenon for the ionosphere, then special methods of TID separation methods should be developed.

Acknowledgement

The present work was done under support of the Russian fund of basic research (Grant No. 06-05-64577).

References

Ahmadov, R.R., Kunitsyn, V.E. Simulation of generation and propagation of acoustic gravity waves in the atmosphere during a rocket flight. Int. J. Geomag. Aeronomy 5 (2), GI2002, doi:10.1029/2004GI000064, 2004.

Hines, C.O. Internal gravity waves at ionospheric heights. Can. J. Phys. 38, 1441–1481, 1960.

Hocke, K., Schlegel, K. A review of atmospheric gravity waves and travelling ionospheric disturbances: 1982–1995. Ann. Geophys. 14 (9), 917–940, 1996.

Kirchengast, G. Elucidation of the physics of the gravity wave-TID relationship with the aid of theoretical simulations. J. Geophys. Res. 101 (A6), 13353–13368, 1996.

Lanchester, B.S., Nygrén, T., Jarvis, M.J., Edwards, R. Gravity wave parameters measured with EISCAT and Dynasonde. Ann. Geophys. 11 (10), 925–936, 1993.

Ma, S.Y., Schlegel, K., Xu, J.S. Case studies of the propagation characteristics of auroral TIDs with EISCAT CP2 data using maximum entropy cross-spectral analysis. Ann. Geophys. 16 (2), 161–167, 1998.

Oliver, W.L., Fukao, S., Sato, T., Tsuda, T., Kato, S., Kimura, I., Ito, A., Saryou, T., Araki, T. Ionospheric incoherent scatter measurements with the middle and upper atmosphere radar: observations during the large magnetic storm of February 6–8, 1986. J. Geophys. Res. 93 (A12), 14649–14655, 1988.

Reinisch, B.W., Huang, X. Calculation of electron density profiles from digital ionograms, 3, processing of bottomside ionograms. Radio Sci. 18 (3), 477–492, 1983.

Reinisch, B.W., Huang, X. Vertical electron content from ionograms in real time. Radio Sci. 36 (2), 335–342, 2001.

Reinisch, B.W., Haines, D.M., Bibl, K., Galkin, I., Huang, X., Kitrosser, D.F., Sales, G.S., Scali, J.L. Ionospheric sounding support of OTH radar. Radio Sci. 32 (4), 1681–1694, 1997.

Reinisch, B.W., Galkin, I.A., Khmyrov, G., Kozlov, A., Kitrosser, D.F. Automated collection and dissemination of ionospheric data from the digisonde network. Adv. Radio Sci. 2, 241–247, 2004.

Shpynev, B.G. Incoherent scatter Faraday rotation measurements on a radar with single linear polarization. Radio Sci. 39 (3), RS3001, doi:10.1029/2001RS002523, 2004.

Williams, P.J.S., van Eyken, A.P., Bertin, F. A test of the Hines dispersion equation for atmospheric gravity waves. J. Atmos. Solar-Terrestrial Phys. 44 (7), 573–576, 1982.

Zherebtsov, G.A., Zavorin, A.V., Medvedev, A.V., Nosov, V.E., Potekhin, A.P., Shpynev, B.G. The Irkutsk incoherent scattering radar. J. Commun. Technol. Electron. 47 (11), 1222–1228, 2002.